Microwave Breakdown in Air, Oxygen, and Nitrogen*

A. D. MacDonald,† D. U. Gaskell,‡ and H. N. Gitterman
General Telephone and Electronics Laboratories Incorporated, Palo Alto, California
(Received 7 January 1963)

The electric fields required to initiate breakdown in air, in nitrogen, and in oxygen have been measured at frequencies in the L, X, and K bands, in a number of resonant cavities. The sizes of the cavities varied greatly so that the relative roles of diffusion and attachment in the breakdown process could be studied. The pressures at which measurements were made varied from approximately 0.01 to 100 mm Hg, corresponding to atmospheric breakdown at altitudes from 15 to 80 km. Pulsed power measurements were made at all frequencies and continuous wave (cw) measurements were made at X and L bands. A theoretical analysis provides a scheme for predicting pulsed and cw breakdown in air for frequencies from 100 Mc/sec to 100 kMc/sec, for pressures corresponding to altitude variation from 0 to 100 km.

INTRODUCTION

THERE has recently been considerable interest in the high-frequency electrical fields required to initiate breakdown in air at high altitudes. Since the pioneering work of Herlin and Brown,[1] however, most of the microwave breakdown studies have been concerned with hydrogen and the noble gases, which are easier to deal with both theoretically and experimentally. There have been some measurements of air breakdown at frequencies of about 3000 Mc/sec,[2,3] some nonuniform field measurements at approximately 9000 Mc/sec,[4] and some theoretical analysis relating dc measurements to microwave measurements.[5] However, these experiments cover relatively restricted ranges of experimental variables and the theoretical analyses depend heavily on the effective electric field concept. As is explained more fully below, there is some question about the range of usefulness of the effective field concept, and so we set out to make a series of breakdown measurements in air, in oxygen, and in nitrogen, at three widely separated frequencies, for a wide range of pressure variation and container size.

The breakdown electric field was measured in five X-band cavities (9.4 kMc/sec), three L-band cavities (992 Mc/sec), and one K-band cavity (24 kMc/sec). These cavities varied in size so that the characteristic diffusion length, Λ, ranged from 0.093 to 2.65 cm. With the exception of some X-band cavities, all cavities were cylindrical and resonant in the TM_{010} mode. The ratio of the height to the radius was such that the electric field could be considered uniform in the region in which breakdown took place. This also implied that the characteristic diffusion length, Λ, is very close to L/π, where L is the cavity height. The two largest X-band cavities were resonant in the TM_{030} mode. The range of pressure variation was not the same for all cavities and was limited by the microwave power available. Pressures reported throughout this paper refer to 20°C. The particle density is actually the important variable in breakdown phenomena, but pressure is retained as the variable in order to facilitate comparison with earlier work. A pressure of 1 mm Hg actually means a number density of 3.29×10^{16} molecules/cc.

EXPERIMENTAL ARRANGEMENTS

The experimental arrangements were essentially the same as those in previous microwave breakdown measurements.[6,7] There were, however, some modifications introduced in order to handle the atmospheric gases, and there was some improved instrumentation. The cavities were made of OFHC copper and were plated with rhodium in order to prevent oxidation and corrosion of the cavity walls by the products of breakdown. All cavities were made in such a manner that they could be baked as part of the vacuum system. Microwave power was measured by means of a Hewlett-Packard calorimetric power meter which was more accurate than the thermistor systems used in earlier measurements. Temperature control of the cavities by water cooling was found necessary when high-power levels were used. The power was coupled by loops to the L-band cavities and by irises to the X- and K-band cavities.

Pure dry air, supplied in one-liter Pyrex flasks by the Linde Corporation, was used for the air breakdown measurements and spectroscopically pure gases, obtained from Linde Corporation and Air Reduction Corporation, were used for the oxygen and nitrogen measurements. It was found that it was not necessary to bake the system after each flask of gas had been used, and it was also found possible to use McLeod gauges, isolated from the cavities by liquid-argon traps, to make the pressure measurements.

* This work was supported in part by the U. S. Air Force under Contract AF 30(602)-2501 for the Rome Air Development Center, Griffiss Air Force Base, New York.
† Present address: Dalhousie University, Halifax, Nova Scotia, Canada.
‡ Present address: Hycon Manufacturing Company, Monrovia, California.
[1] M. A. Herlin and S. C. Brown, Phys. Rev. **74**, 291 (1948).
[2] L. Gould and L. W. Roberts, J. Appl. Phys. **27**, 1162 (1956).
[3] D. J. Rose and S. C. Brown, J. Appl. Phys. **28**, 561 (1957).
[4] P. Platzman and E. H. Solt, Phys. Rev. **119**, 1143 (1960).
[5] S. C. Brown, in *Handbuch der Physik*, edited by S. Flügge (Springer-Verlag, Berlin, 1956), p. 531.
[6] A. D. MacDonald and S. C. Brown, Phys. Rev. **75**, 411 (1949).
[7] A. D. MacDonald, D. M. Fraser, H. Bradford, and G. F. O. Langstroth, Can. J. Phys. **37**, 1166 (1959).

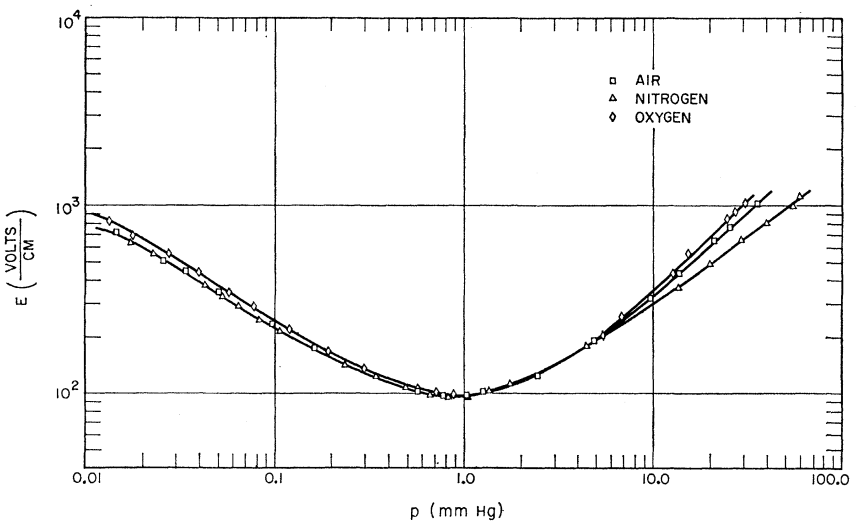

FIG. 1. Cw breakdown fields in air, oxygen, and nitrogen at a frequency of 992 Mc/sec. (Characteristic diffusion length $\Lambda = 0.631$ cm.)

The experimental arrangements for K-band measurements were slightly different from those for X band and L band. It was found that it was possible to use a high-power attenuator along with a calibrated variable attenuator to replace the power divider. This resulted in some improvement in measuring technique.

We made cw measurements on all the L-band and X-band cavities but did not have sufficient power to make cw measurements on the K-band cavity. The maximum error in the cw measurements was estimated to be 2%, although variation in the breakdown fields, measured at different times and with different gas samples, was less than 1%.

Breakdown fields were measured for pulsed power on one L-band, two X-band, and one K-band cavity. When making the pulsed power measurements it is necessary to specify what we mean by breakdown. We define the pulse breakdown threshold as the least electric field, which, when it exists for the duration of the pulse, is great enough so that sparking is initiated by the time the pulse ends. This breakdown field was measured by displaying the power transmitted through the cavity on an oscilloscope and noting that power level at which transmission was blocked during the last 5% of the pulse width. In order to get reproducible results for pulse breakdown it is necessary that during the time of the pulse there be some electrons in the volume in which the maximum electric field exists. We found it necessary to have a 5-mCi cobalt-60 gamma-ray source next to the cavities to produce sufficient ionization to get repeatable results for the pulsed work, although a 5 μCi source had sufficed for the cw work. In other words, it was necessary for us to insure that the statistical time lag was substantially smaller than the pulse width. The estimated error in the pulse breakdown measurements at L band and X band is about 10% although the

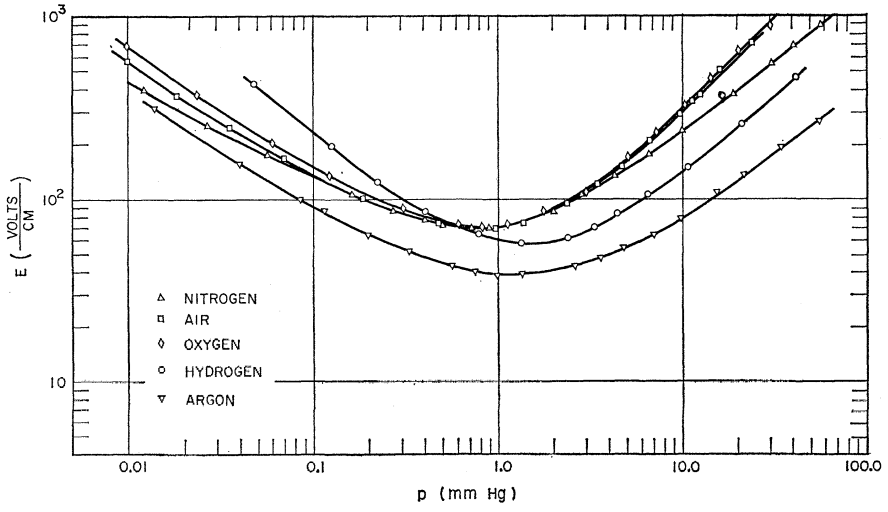

FIG. 2. Cw breakdown fields in nitrogen, oxygen, air, hydrogen, and argon at a frequency of 994 Mc/sec. (Characteristic diffusion length $\Lambda = 1.51$ cm.)

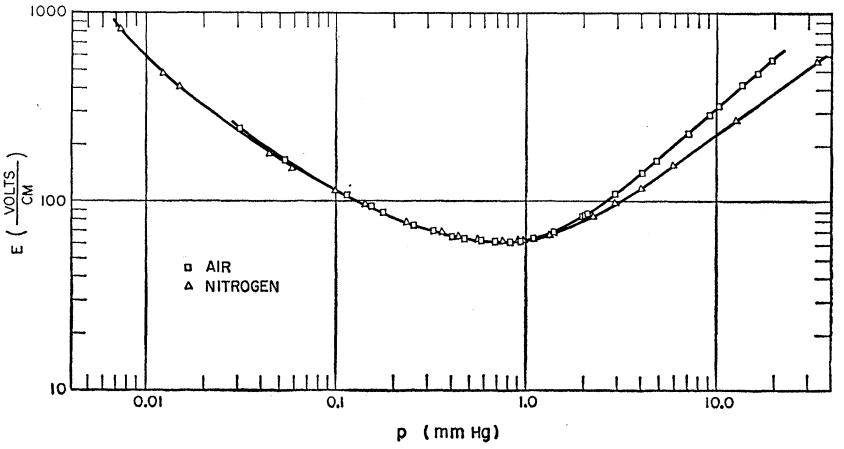

FIG. 3. Cw breakdown fields in air and nitrogen at a frequency of 994 Mc/sec. (Characteristic diffusion length $\Lambda = 2.65$ cm.)

data for the longer pulse lengths are somewhat more accurate. The over-all accuracy of the K-band measurements is estimated at approximately 15%. The pulse-forming networks and the associated power supply were designed to ensure that the rise time and the fall time of the pulse were very short compared with the pulse length.

EXPERIMENTAL DATA

Figures 1, 2, and 3 present the cw breakdown electric fields as a function of pressure as measured at 994 Mc/sec in cavities of characteristic diffusion lengths 0.631, 1.51, 2.65 cm. All electric fields reported refer to rms values. Breakdown fields in air and in nitrogen were measured for all three cavities and in oxygen for two cavities. Measurements taken in hydrogen and in argon for one cavity are also shown. In Fig. 4 the data for air for the three cavities are compared to show the effect of diffusion on breakdowns.

Figures 5, 6, and 7 show cw breakdown fields at 9.4 kMc/sec for air, nitrogen, and oxygen, and in one case also for hydrogen, in cavities of characteristic diffusion lengths 0.103, 0.220, and 0.400 cm. In Fig. 8 is shown a comparison of the air breakdown data for these cavities, as well as for the larger TM_{030} mode cavities of characteristic diffusion lengths 0.64 and 1.29 cm. In Figs. 8 and 4 actual experimental points are omitted in order to illustrate the effect of diffusion more clearly. It is to be noted that the uppermost curve in Fig. 8 shows an inflection point at a pressure of about 0.3 mm of mercury. In this cavity at the lower pressures the mean free path of the electrons becomes comparable to the cavity height, and one would not expect diffusion theory to describe the processes in this case. The arrow above the breakdown curve for the smallest cavity indicates approximately the pressure at which one would expect some change to take place because of this effect.

The data for pulse power breakdown in air are shown in Fig. 9 for one L-band cavity and in Figs. 10 and 11 for two X-band cavities. The theoretically determined curves in these figures will be discussed. Figure 12 shows the pulse-breakdown fields in air for several pulse

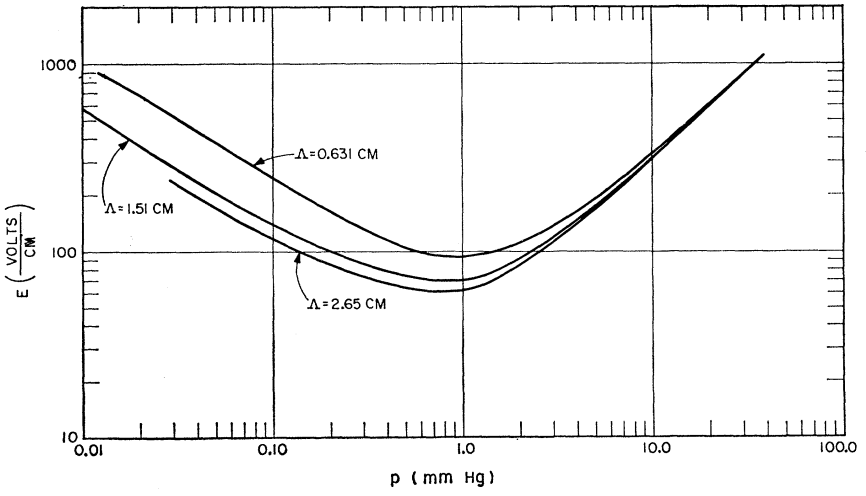

FIG. 4. Cw breakdown fields in air for three L-band cavities.

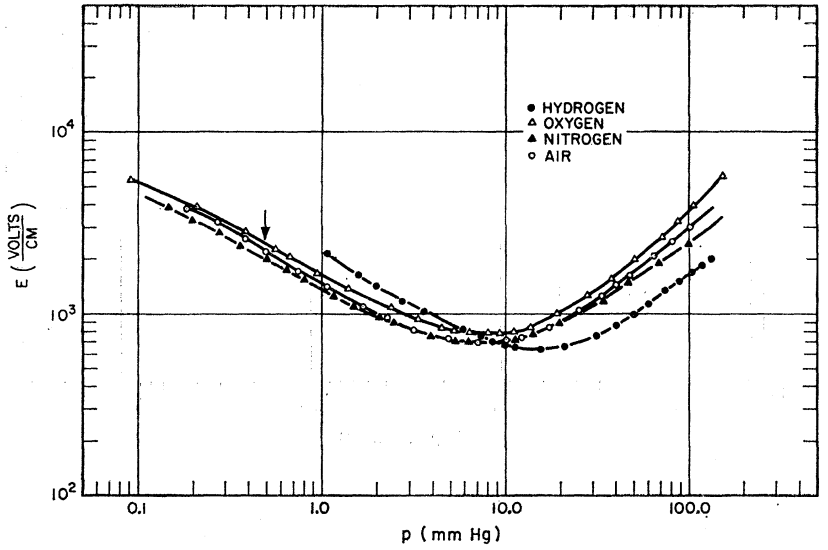

FIG. 5. Cw breakdown fields for air, oxygen, nitrogen, and hydrogen at a frequency of 9.4 kMc/sec. (Characteristic diffusion length $\Lambda=0.103$ cm.)

lengths and a frequency of 24.1 kMc/sec. The breakdown fields in nitrogen are not shown in this figure but they were found to be within about 10% of the air breakdown values at pressures above 100 mm Hg and practically indistinguishable from them at pressures below 80 mm Hg.

DISCUSSION

In some previous breakdown studies it has been possible to analyze the probelm theoretically by solving the Boltzmann equation for the electron velocity distribution function and calculating the appropriate electron production and loss mechanisms to arrive at an equation relating breakdown fields with pressures and other experimental parameters.[6,8,9] In those cases in which the electron-atom collision frequency could be considered independent of electron energy, the theoretical analysis was made particularly simple by the introduction of an effective electric field. An examination of a simplified version of the Boltzmann transport equation makes clear the genesis and also the limitations of the effective field concept. The Boltzmann equation for electrons whose energy is less than that of the lowest excitation level of the gas atoms may be written

$$E^2\Lambda^2\nu_c\frac{d}{du}\left[u^{3/2}\frac{\nu_c}{\nu_c^2+\omega^2}\frac{df}{du}\right]+\alpha\Lambda^2\nu_c\frac{d}{du}(\nu_c u^{3/2}f)-u^{3/2}f=0, \quad (1)$$

where E is the rms value of the electric field, Λ is the characteristic diffusion length, ν_c is the frequency of collision of electrons with neutral particles, u is equal to the electron energy, ω is 2π times the frequency of the applied field, α is a constant made up to the charge and mass of electrons and atoms, and f is the electron energy distribution function. The right-hand side is no longer zero when the electron energy is above that necessary for excitation, but the present argument is not changed by this fact.

If ν_c is independent of energy, the equation may be simplified and the frequency dependence put in one term by letting

$$E_e^2=\frac{E^2}{1+(\omega^2/\nu_c^2)};$$

then Eq. (1) becomes

$$E_e^2\Lambda^2\frac{d}{du}\left[u^{3/2}\frac{df}{du}\right]+\alpha\nu_c^2\Lambda^2\frac{d}{du}(u^{3/2}f)-u^{3/2}f=0. \quad (2)$$

For this particular case, then, the effective field concept is particularly useful in making possible a description of the breakdown properties of the gas by means of a single curve relating $E_e\Lambda$ and $p\Lambda$. The distribution function can also be found for this case and calculation of breakdown made in such a way that breakdown fields can be predicted with some confidence over a large range of variation of experimental parameters.

Unfortunately, the electron-molecule collision frequency in air is very strongly energy-dependent, as can be seen from the data collected by Brode.[10,11] Therefore, the simplified analysis cannot be made in this case. We have made attempts, as have others, to find an

[8] A. D. MacDonald and S. C. Brown, Phys. Rev. **76**, 1634 (1949).
[9] W. P. Allis and S. C. Brown, Phys. Rev. **87**, 419 (1952).
[10] R. B. Brode, Rev. Mod. Phys. **5**, 257 (1933).
[11] S. C. Brown, *Basic Data on Plasma Physics* (John Wiley & Sons, Inc., New York, 1958), p. 8.

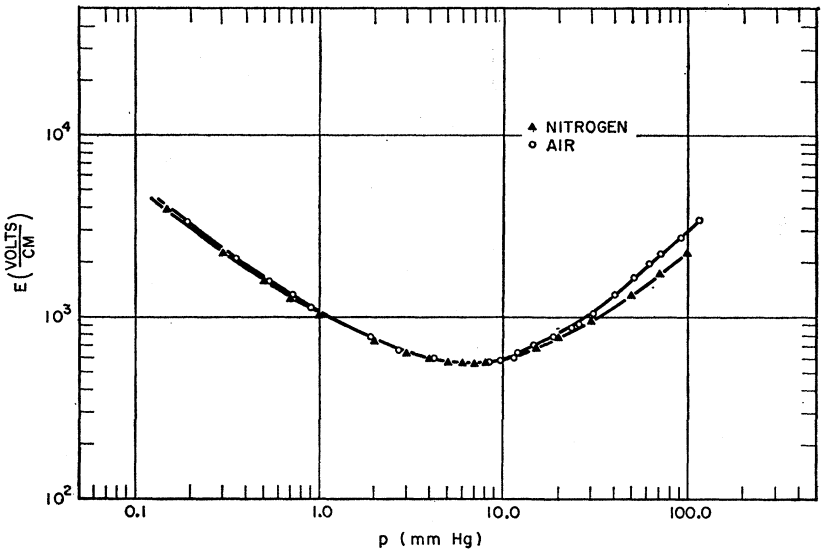

FIG. 6. Cw breakdown fields for air and nitrogen at a frequency of 9.4 kMc/sec. (Characteristic diffusion length $\Lambda=0.22$ cm.)

average collision frequency which would present all the data in a single curve. Figure 13, which includes our data and some of that from Herlin and Brown, shows that this cannot readily be done for air. In this calculation we have used a value of $5.3\times10^9\ p$ (p in mm Hg) for the collision frequency ν_c. In those cases in which the characteristic diffusion length is relatively small compared with the free-space wavelength of the electric field, λ, the experimental data thus far obtained lie fairly close to a single curve, and for some purposes this single curve is a sufficiently accurate description. However, as will be noticed from the figure, for large Λ and small $p\Lambda$ there is no single curve which fits all the data. It should be pointed out that for Λ large enough so that $p\Lambda$ is above 10 cm mm Hg, all curves for all frequencies and container sizes form a single straight line, giving a ratio of $(E_e\Lambda/p\Lambda)$ of approximately 30 V/cm mm Hg. If the product $p\lambda$ is large enough (greater than 100 cm mm Hg) then E and E_e are approximately the same so that from this curve we can get a value of the breakdown field and power appropriate when microwave energy is radiated into very large volumes. However, since these are somewhat restricted conditions, we have devised an alternative representation which does not use the effective field except in an indirect way and, therefore, provides a more accurate description of the experimental data. This does not represent a theory in the same sense as the theoretical analyses which have been carried out for helium, hydrogen, neon, and argon; but, at the same time, it does use some of the basic ideas of these theories and presents in an empirical manner a method for calculating breakdown fields for

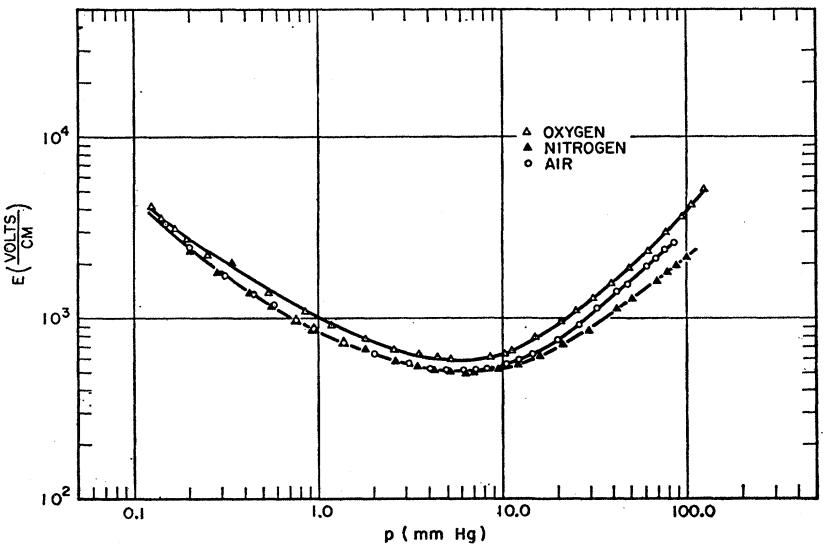

FIG. 7. Cw breakdown fields for air, oxygen, and nitrogen at a frequency of 9.4 kMc/sec. (Characteristic diffusion length $\Lambda=0.40$ cm.)

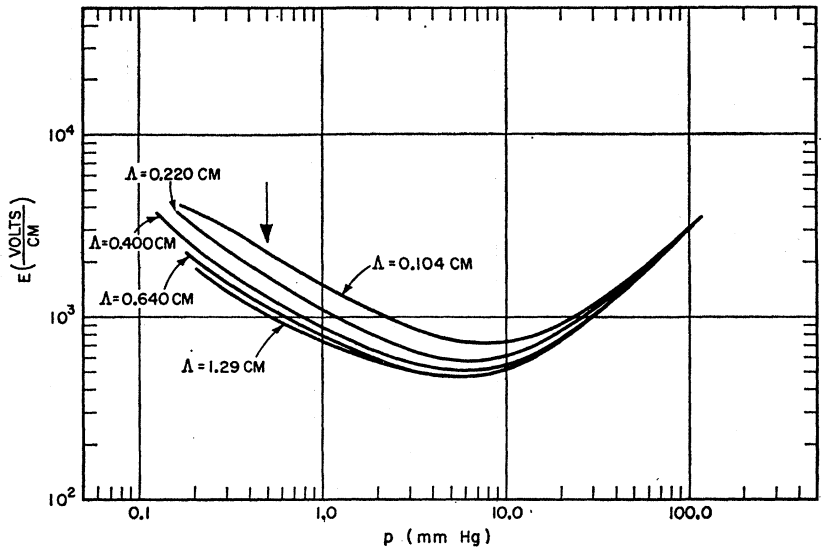

FIG. 8. Cw breakdown in air in several cavities at a frequency of 9.4 kMc/sec. (Arrow indicates pressure at which mean free path is approximately equal to cavity height.)

a very large variety of conditions. Also, as will be shown, the method can be used for pulsed as well as cw processes.

The two most important processes whereby electrons are lost to the discharge in air are diffusion and attachment. Recombination is relatively unimportant because of the low-electron density existing before breakdown. We represent by ν_a the attachment rate and by ν_i the ionization rate, and we may write the breakdown condition as follows:

$$\nu_i = \nu_a + (D/\Lambda^2). \tag{3}$$

The term D/Λ^2 is the rate at which electrons are lost by diffusion. If we knew the diffusion coefficient, D, under all conditions, we could find a direct value for the net ionization rate, $\nu_i - \nu_a$, from a set of experimental breakdown data.

The value of D has not been measured for conditions of high electric fields in air. The values of D will, of course, depend on the electric field, on the pressure, and on the nature of the electron velocity distribution function. A calculation of the product D multiplied by the pressure has been made for the cases of Maxwellian and Druyvesteyn distribution functions under certain assumptions as to the collision cross sections. Subject to these approximations, which have been found to be reasonably good, the diffusion coefficient may be written in the following way:

$$Dp = 3.2 \times 10^5 \bar{u} \quad (\text{cm}^2 \text{ mm Hg/sec}), \tag{4}$$

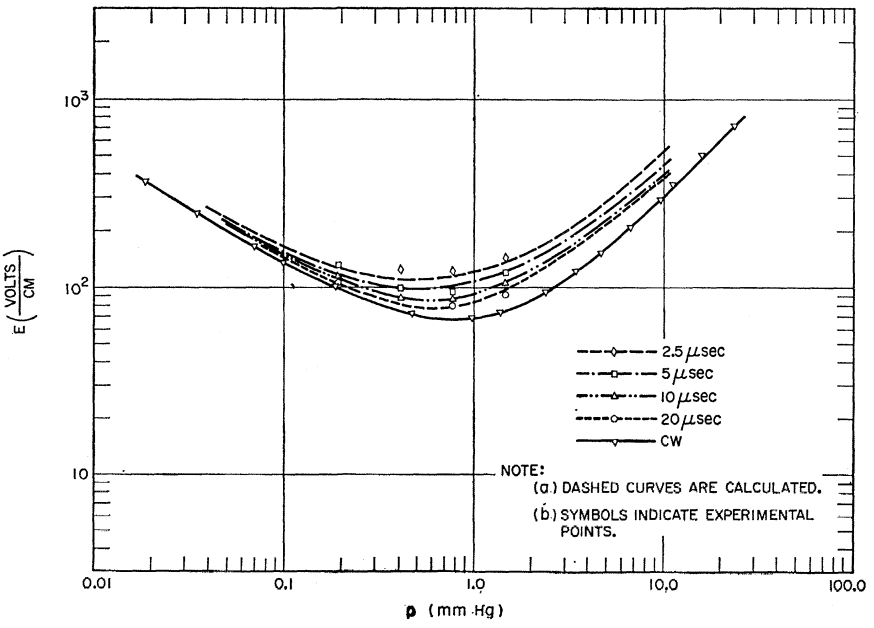

FIG. 9. Cw and pulsed breakdown fields in air at a frequency of 994 Mc/sec. (Characteristic diffusion length $\Lambda = 1.51$ cm.)

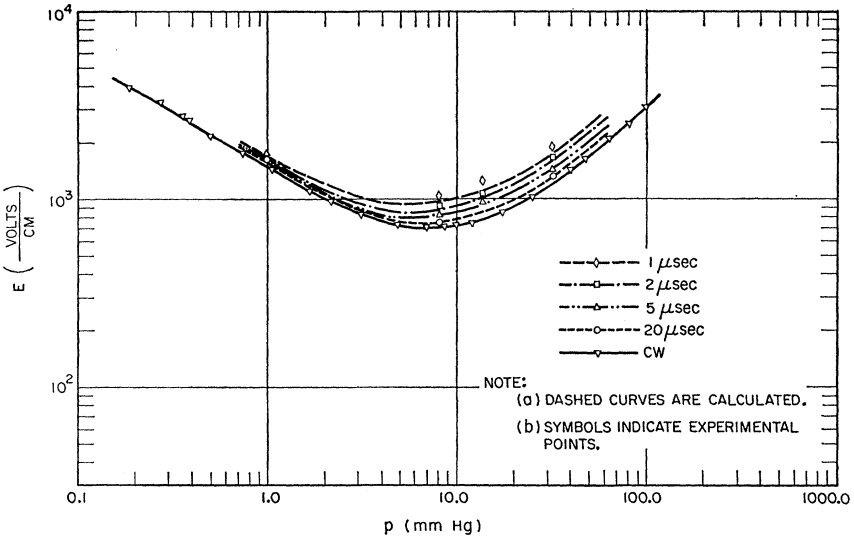

FIG. 10. Cw and pulsed breakdown fields in air at a frequency of 9.3 kMc/sec. (Characteristic diffusion length $\Lambda=0.10$ cm.)

where $\bar{u}$ is the average electron energy in volts.[12] Values of the average electron energy have not been measured for high-electric fields. However, Crompton, Huxley, and Sutton have made measurements of the average electron energy in air for values of E/p up to about 25 (V/cm mm Hg).[13] For values of E/p above about 5 (V/cm mm Hg), these data show that the average electron energy is directly proportional to E/p, and we assume that the proportionality continues to higher values of E/p. We now make use of the effective field idea and assume that for high frequencies the average energy of electrons will depend upon the effective field rather than the actual value of the field. Using the straight line extrapolation of these data combined with Eq. (4), there results

$$Dp=[29+0.9(E_e/p)]10^4 \quad (\text{cm}^2 \text{ mm Hg/sec}), \quad (5)$$

where the units of E_e are V/cm and of p, mm Hg.

As pointed out above, at breakdown $\nu_i-\nu_a=D/\Lambda^2$. Using the value of D from Eq. (5) we can calculate a series of curves showing the net ionization, $\nu_i-\nu_a$, as a function of $p\lambda$ for different values of $E\lambda$. We make this calculation by taking the breakdown data and manipulating them in the following manner. For a given value of breakdown field at a particular pressure, as determined from the breakdown curves, we calculate Dp from Eq. (5), multiply it by $(\lambda/\Lambda)^2$, and divide by $p\lambda$. This then gives the product $D\lambda/\Lambda^2$, which at breakdown is

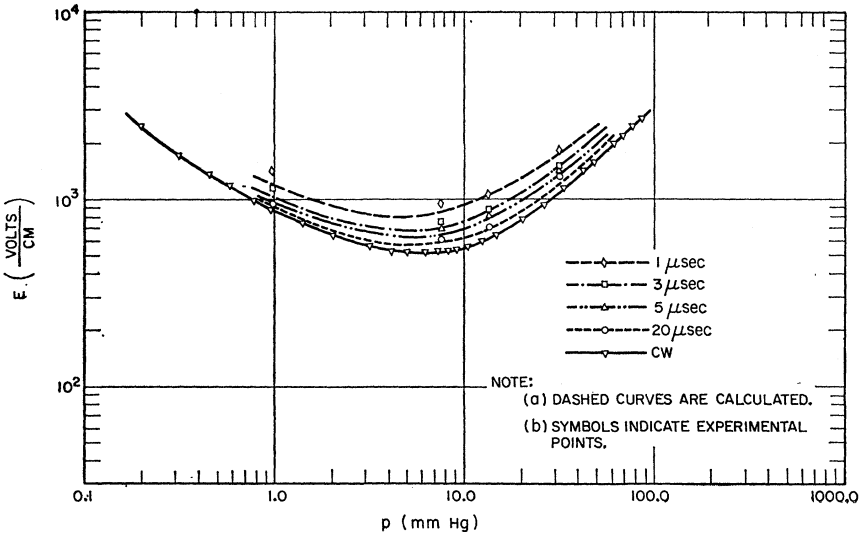

FIG. 11. Cw and pulsed breakdown fields in air at a frequency of 9.3 kMc/sec. (Characteristic diffusion length $\Lambda=0.40$ cm.)

[12] A. D. MacDonald, Proc. I.R.E. 48, 436 (1959).
[13] R. W. Crompton, L. G. H. Huxley, and D. J. Sutton, Proc. Roy. Soc. (London) A218, 507 (1953).

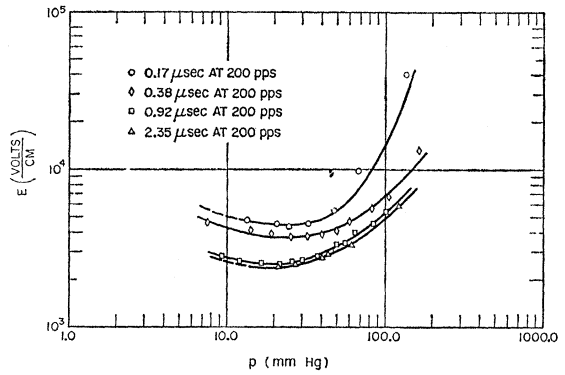

FIG. 12. Pulsed breakdown fields in air at a frequency of 24.1 kMc/sec. (Characteristic diffusion length $\Lambda=0.09$ cm.)

equal to $\nu\lambda$. Proceeding in this manner we can construct a series of curves which are shown in Fig. 14.

We can write $D\lambda/\Lambda^2$ alternatively in a slightly different manner by taking the value for Dp from Eq. (5), multiplying by $(\lambda/\Lambda)^2$, and dividing by $p\lambda$. This results in the following equation:

$$D\lambda/\Lambda^2=10^4(\lambda/\Lambda)^2S, \tag{6}$$

where S is given by

$$S=(1/p\lambda)\{29+0.9E\lambda/[(p\lambda)^2+(35.6)^2]^{1/2}\}. \tag{7}$$

The term S is plotted in Fig. 15 for a number of different values of $E\lambda$, as a function of $p\lambda$.

If we were now to plot this curve on transparent graph paper, we could see that by multiplying the line where $S=1$ by the factor $10^4(\lambda/\Lambda)^2$ we would have the values of $D\lambda/\Lambda^2$ plotted as a function of $p\lambda$. We can then superpose this on our previous graph. The intersection of the lines of the same $E\lambda$ from two graphs indicates a combination of variables appropriate to breakdown. It can thus be readily seen that by combining these two curves we can extract breakdown data for a great variety of conditions. For example, if we have a known frequency and a known container size, we can immediately determine at what vertical height on Fig. 14 we set Fig. 15; and immediately we have the values of $E\lambda$ and $p\lambda$ for breakdown conditions. It is then a simple matter to construct an E-p breakdown curve.

The data from which these graphs were compiled include all the cw data shown in Figs. 1 through 11 at frequencies of 1, 9.4, and 24 kMc/sec, as well as the data of Rose and Brown.[4]

THEORETICAL ANALYSIS OF PULSED DATA

One considerable advantage of the method of presentation of the breakdown curves employed in the previous section is that Fig. 14 can be readily adapted to calculations of pulsed breakdown. When an electric field is applied to a gas for a very short period of time the process which goes on is essentially the same as that which happens when we are considering cw breakdown. However, there is a short period of time when the pulse is initially applied which is required for the electron concentration to increase, i.e., the formative time lag. During this period of time the electron concentration is given as a function of time by the equation

$$n=n_0e^{\nu t}. \tag{8}$$

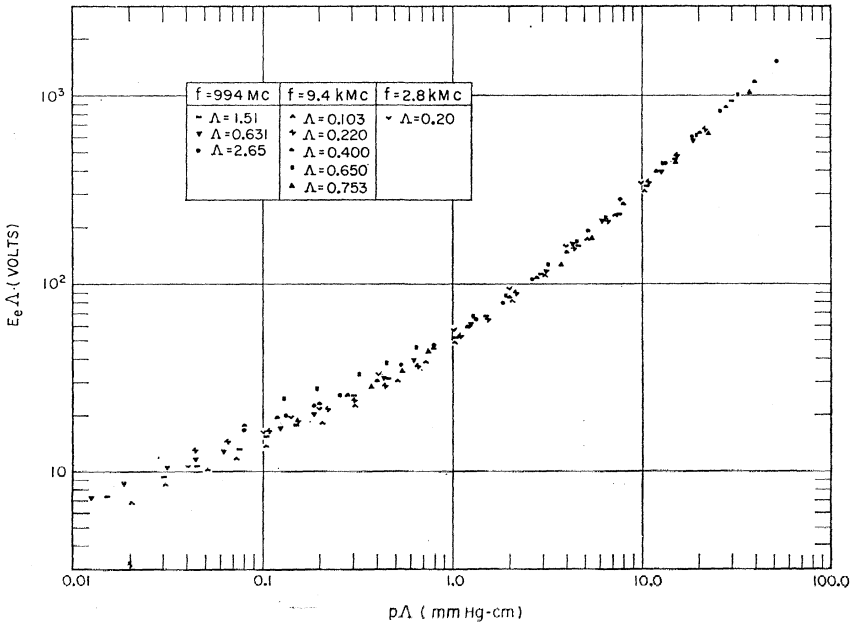

FIG. 13. $E_e\Lambda$ as a function of $p\Lambda$ for several cavities, assuming $\nu_c=5.3\times10^9p$.

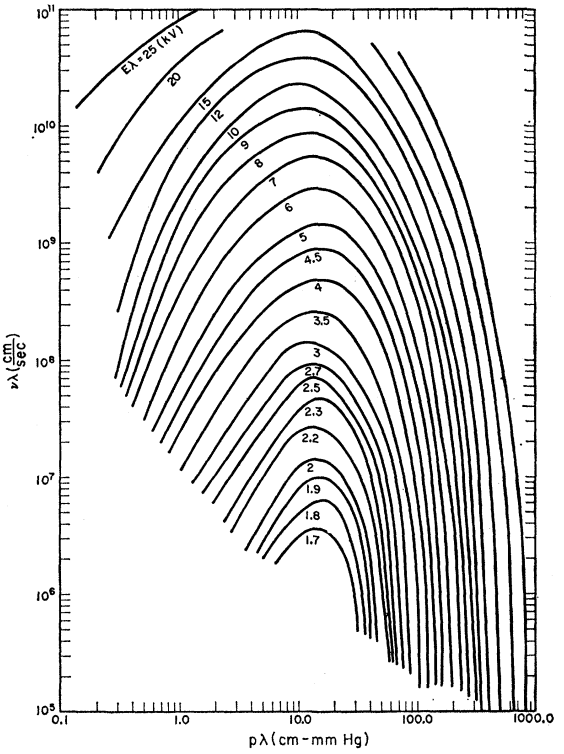

FIG. 14. $\nu\lambda$ as a function of $p\lambda$ for constant $E\lambda$.

In this equation the ν means the net ionization rate; in other words, in the case of air ν is equal to $\nu_i-\nu_a-(D/\Lambda^2)$. It is, therefore, a measure of the excess of the production rate of electrons over the loss rate.

Breakdown takes place for pulsed conditions if the electron concentration reaches the plasma concentration value by the end of a given pulse. We assume for the purposes of this calculation that the time between pulses is sufficiently long so that there is no large number of electrons left over from one pulse to influence the next. We may, therefore, set as a criterion for breakdown the condition that

$$n_p=n_0e^{\nu\tau}, \tag{9}$$

where n_p is the plasma concentration, which is equal to $10^{13}/\lambda^2$ (λ is the wavelength in centimeters), if the concentration is measured in number of particles/cc and τ is the pulse length.

The initial concentration of electrons is not accurately known; however, because of the exponential nature of the phenomenon, the results which one obtains by varying the initial electron concentration between $1/cm^3$ and $1000/cm^3$ are not very different. The 5-mCi cobalt-60 source which was used produced in most of the cavities an electron concentration of approximately 100 electrons/cc. In the absence of an electron from a radioactive source, the breakdown fields are considerably larger because it may very well happen that during the relatively small fraction of time that the electric field is on, natural cosmic radiation will not produce any electron within the region where the electric field is large. In applying the results of these experiments to breakdown in the atmosphere, one must be careful to realize that breakdown will not take place at all if there are no electrons to provide the initial ionization within the region in which the electric field is applied. Therefore, the pulsed breakdown conditions which we derive are in the nature of a lower limit to the field or power which is required to produce breakdown.

We use Fig. 14 directly to calculate breakdown fields in the following manner. Given the cavity size, which gives us Λ, we first calculate the value of D/Λ^2, which we can do by estimating the breakdown field to obtain the value of D from Eq. (5). We use Eq. (9) and find out what value of $\nu\tau$ is required to produce plasma concentration for the wavelength under consideration and then, knowing the pulse length, we can calculate the ν. The ν of Fig. 14 is equal to $\nu_i-\nu_a$; but, knowing the net ν and D/Λ^2, we can calculate ν and $\nu\lambda$. Then, knowing $p\lambda$, we can read off directly the product $E\lambda$. In Figs. 10 and 11 are shown the results of calculations by this procedure for pulsed breakdown in a cavity at X band with pulses of various durations and with a repetition rate of 1000/sec. The dashed lines are the calculations predicted from this curve; the points are the experimental measurements. Similar calculations and experiments for L band are shown in Fig. 9. Except at the very short pulse lengths where the pulse

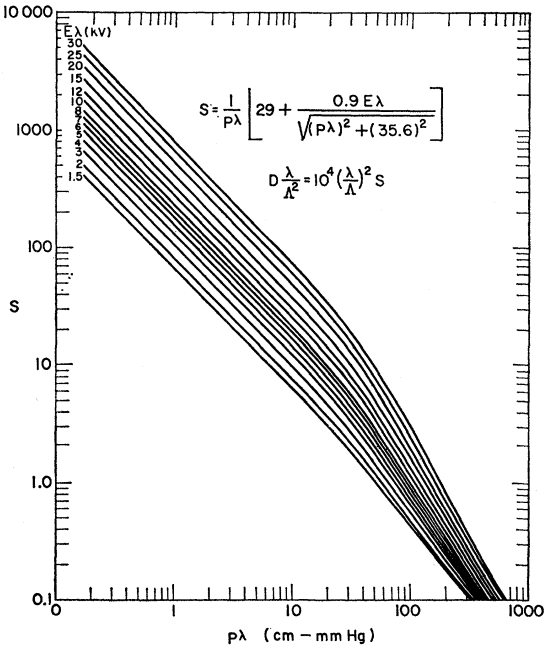

FIG. 15. $(D\lambda/\Lambda^2)$ as a function of $p\lambda$ for constant $E\lambda$.

length is not well known, there is remarkable agreement between the calculations and the measured points.

The authors consider it likely that the use of Figs. 14 and 15 enable one to predict with reasonable assurance the pulsed and cw properties of air for frequencies from 100 Mc/sec to 100 kMc/sec over a range of pressure corresponding to an altitude variation of from 0 to 100 km, and over a very wide range of variation of container sizes.

PHYSICAL REVIEW VOLUME 130, NUMBER 5 1 JUNE 1963

Theory of Stimulated Raman Scattering

R. W. HELLWARTH
Hughes Research Laboratories, Malibu, California
(Received 22 October 1962)

Relations which describe the gain that is produced by the stimulated Raman scattering of intense light in a Raman-active material are developed entirely in terms of measurable material parameters (such as the ordinary Raman scattering cross sections). It is this gain which must overcome propagation losses in order to achieve the laser action that has been observed from this effect. Expressions for the gain are derived for scattering material either in thermal equilibrium or in certain nonequilibrium conditions. The dynamical equations governing the time behavior of the Raman-laser light are discussed.

WHEN various Raman-active liquids are placed inside an optical Fabry-Perot cavity and illuminated by light of frequency ω_α and intensity greater than a certain threshold, then coherent light builds up in the cavity at a frequency(s) ω_β which equals ω_α minus the frequency of a Raman-active vibration.[1,2] There is no (or negligible) resonant absorption at ω_α; all evidence indicates that stimulated Raman scattering is causing laser action.[2] Javan has proposed that a two-level Raman maser would be possible with no quantum states available other than an initial and final matter state[3]; he and Weber have calculated the rate at which such a two-level process would proceed.[3,4] However, the optical effect of interest here involves the normal Raman process with the mediation of large numbers of intermediate quantum states; the calculation of the matrix elements for this case would be extremely difficult. Therefore, we will content ourselves here with the development of a phenomenological theory to describe stimulated Raman scattering in terms of tabulated or measurable material parameters, namely ordinary Raman scattering cross sections. This treatment will be analogous to the treatment of ordinary lasers on the basis of absorption and fluorescence data.

The Raman process consists of (not necessarily in this order) annihilating a photon from a radiation mode α and creating a photon in another mode β (of different frequency), the energy difference being taken up by a transition in the scattering matter from a state i (of energy ϵ_i) to a state j (of energy ϵ_j) with $\epsilon_i+\hbar\omega_\alpha=\epsilon_j+\hbar\omega_\beta$. Unlike the case of fluorescence, there is no real intermediate state in this process which conserves energy. The possibility of laser action, or material gain, at ω_β arises from the values of the matrix elements for creating and annihilating photons. These matrix elements contribute a factor $n_\alpha(1+n_\beta)$ to the rate at which the process described above proceeds and a factor $n_\beta(1+n_\alpha)$ to the reverse process; n_α and n_β are the number of photons present in the incident and scattered modes, respectively. If we are considering the scattering of plane waves, then α represents the wave vector and polarization of the incident or pump radiation, β refers similarly to the scattered wave, which, by virtue of the term in the rate which is proportional to n_β, may become a growing wave in the pumped medium. When it is more convenient, α and β may refer to standing wave modes in a cavity; we will consider both cases. The scattering rate has, in addition to the factors mentioned above, a factor depending on matrix elements between various states in the medium $S_{ij}(\alpha,\beta)$ which also depends parametrically on ω_α and ω_β and on the spatial shapes of the modes α and β. Suppose the matter has probabilities P_i of being in the ith state. Then the average net rate of change of photon number in the scattered mode β arising from a given matter transition and incident mode α, is of the form

$$\dot{n}_\beta=n_\alpha(1+n_\beta)S_{ij}(\alpha,\beta)P_i-n_\beta(1+n_\alpha)S_{ji}(\beta,\alpha)P_j. \quad (1)$$

In (1) and what follows, the subscript j symbolizes those states for which $\epsilon_i+\hbar\omega_\alpha=\epsilon_j+\hbar\omega_\beta$. If the terms on the right-hand side of (1) which are proportional to n_β are positive, then they represent a contribution to

[1] E. J. Woodbury and W. K. Ng, Proc. I. R. E. **50**, 2367 (1962).
[2] Gisela Eckhardt, R. W. Hellwarth, F. J. McClung, S. E. Schwarz, D. Weiner, and E. J. Woodbury, Phys. Rev. Letters **9**, 455 (1962).
[3] A. Javan, Bull. Am. Phys. Soc. **3**, 213 (1958); J. Phys. Radium **19**, 806 (1958).
[4] J. Weber, Rev. Mod. Phys. **31**, 681 (1959).